A Novel Grid Support Topology using Nine Switch Converter for Offshore Connected Wind Farms

M. Keerthiga [1], M. Nithya [2], S. Preerthi [3], Dr. R. Ilango [4], G. Purushothaman [5]
(BE(Electrical And Electronics Engineering),M.A.M School of Engineering, Tiruchirapalli,Tamilnadu, India)[1,2,3]
(Prof[4],Asst.Prof[5] Department of EEE ,M.A.M School of Engineering, Tiruchirapalli,Tamilnadu,India)

Abstract: **This paper proposes Nine Switch Converter (NSC)based configuration and control strategy for the VSC-HVDC connected offshore WFs to enhance the Fault Ride Through(FRT) operation of the system. The configuration allows having both shunt and series interfaces to the onshore grid, which allows the isolation of the faulty part of the network, continuous power delivery to the healthy portion and significant reduction of the fault current. Reduced switch count nine switch converter is utilized at the onshore station to provide simultaneous shunt and series compensation to the electric grid. The proposed control strategy ensures full power evacuation and the DC link voltage regulation during network disturbances. The comparative analysis between the proposed and conventional VSC-HVDC systems carried out in Matlab/ Simulink environment revealed the former's enhanced transient performance.**

INTRODUCTION:

The offshore WFs are becoming increasingly popular due to several advantages over the currently predominant onshore wind farms. By 2030, Europe plans to have an installation of 120 GW offshore wind power out of the expected 300 GW total wind power installation [1]. For the transmission distances over 100 km, the VSC based HVDC systems are considered to be the best solution to transfer offshore wind power to the main onshore grid [2], [3]. One of the most important aspects of the VSC-HVDC connected offshore WF system operation is the wind power evacuation during onshore AC grid faults. During such faults,the whole power supplied by the WF cannot be injected into
the grid as the voltage in the onshore converter terminal experiences dip. The wind power, which is still being delivered to the DC link by the offshore converter, is being accumulated in the DC capacitors. This causes the voltage across those capacitors to rise. If the DC overvoltage exceeds certain threshold (usually 5-10 %), the converter and other equipment
can be significantly damaged.

EXISTING SYSTEM:

Many studies investigated the performance of the VSCHVDC
connected offshore WF system during onshore AC faults. After the detection of the fault based on the DC link voltage rise, [4] suggests blocking converters for a period estimated by the DC link voltage and current deviations from their prefault values. However, even when the IGBT switches of the sending end converter are blocked, the reverse flowing current through antiparallel diodes will cause the power to flow to the DC circuit [2]. For the Doubly Fed Induction Generator (DFIG) based offshore WF connected to the grid through an VSC-HVDC link, [5] suggests a new control strategy to reduce the active power generation in the WF once the DC link voltage exceeds the allowed threshold. For the WFs based on fully rated converters and connected through a VSCHVDC link, two power reduction techniques are suggested in [6]. The first method is to reduce the generated power from each wind turbine upon the onshore fault detection by reducing the torque reference in the turbine side converter. The Second solution presented in [6] is to reduce the sending end converter terminal AC voltage proportional to the DC link Voltage rise. However, the sudden reduction of the offshore grid voltage is seen as a short circuit from the machine side. The turbine may accelerate due to power imbalance. Moreover, large DC current component arising from the sudden voltage reduction may cause stresses on the converters as well as the machine itself. To tackle the later issue, [7] suggested to inject
prespecified DC voltage together with the reduction of the voltage in the offshore grid.

PROPOSED SYSTEM:

In this paper an NSC based FRT strategy for VSC-HVDC connected offshore WFs is developed, which has the following features: It allows simultaneous shunt and series connection to the grid while utilizing fewer switches in comparison with the topology using two separate converters.

- The proposed transient management scheme does not rely on the system reconfiguration, and therefore it avoids an interruption of inductive currents.
- The voltage restoration allows smooth power evacuation from the WF without stresses on the mechanical systems
of the offshore turbines during normal and fault operation of the AC grid. The strategy does not depend on the turbine type.
- The proposed topology restores voltage profile in one portion of the grid and reduces the fault current contribution,
acting as a dynamic fault current limiter.
- The developed control strategy based on the one bus ahead voltage measurement includes the DC link voltage regulation loop. Therefore, DC link voltage control is
ensured without the inclusion of any additional energy evacuation devices such as DC chopper.
- The proposed transient management scheme tackles both balanced and unbalanced fault conditions, avoiding significant power oscillations in the DC side. Moreover,the fast phase detection algorithm namely Frequency Locked Loop (FLL), implemented in this paper for VSCHVDC application, enhances the transient response of the system.

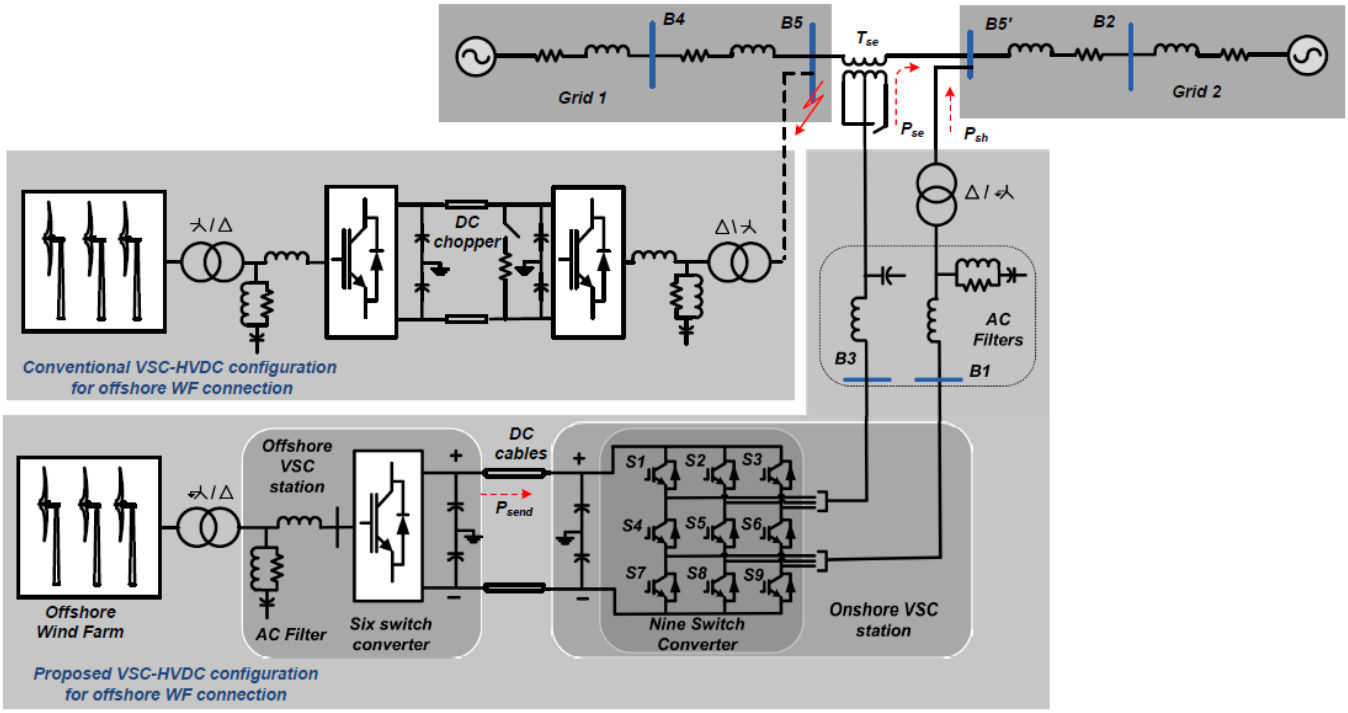

Fig. 1. The conventional configuration vs proposed topology of the VSC-HVDC system for offshore WFs (either of the systems is connected)

II. THE PROPOSED CONFIGURATION OF THE VSC-HVDC:

The single line diagram of the proposed configuration for the wind farm connected to the grid through VSC-HVDC system is shown in Fig.1. Two voltage sources with their The venin impedances are used to represent the equivalent onshore Grid. In the proposed configuration, the conventional six switch converter of the receiving end station is replaced with an NSC. This allows the connection to the main grid via both series and shunt interfaces. The aim of the proposed configuration is to ensure smooth
power evacuation during the fault duration and to protect
the VSC-HVDC system as well as WF turbines from severe
stresses and transients. In addition to that, the provided compensation
prevents the sudden reduction of the power delivered to the electrical grid, which may result in improving the grid security and stability in response to severe fault conditions. It is worthy to note that the studied system does not require DC chopper to dissipate the extra power during AC grid faults. The main extra components needed to reconfigure the original topology into the proposed scheme are the additional
three power electronic switches for deriving the NSC from six switch converter, series LC filter, and the series transformer Tse. Detailed modeling of the onshore station and its connection to the grid through shunt and series interfaces has been performed, which includes the converter station itself with its /Y connected converter transformer, phase reactors,high pass filters, series LC filter and other components as shown in Fig. 1. Second order high pass filters depicted in Fig. 1 are extensively used for HVDC application, which in this study are used to eliminate switching and the double switching frequency harmonic injection to the grid [16], [17].The proposed transient management scheme aims to ensure
the seamless operation on the offshore side of the system during onshore AC grid disturbances. Hence, the sending end
converter injects the rated power into DC link during normal and transient operations. During normal operation, the shunt connection is controlled to maintain the reference DC link voltage and to regulate the B5′ bus voltage. The total active power is delivered to the grid through the shunt terminal.The series transformer is short circuited on the converter side during normal operation. During the grid fault condition,
the series converter provides the voltage across the series transformer in such a way as to isolate the grid fault and to restore the voltage profile in other portion of the grid. Thus,it acts as a dynamic fault current limiter in the electric grid.Also, the voltage restoration allows evacuating the wind power to the healthy portion of the network. The operation of the proposed configuration and control strategy during faults in two different locations on both sides of the series transformer is examined in Section III.

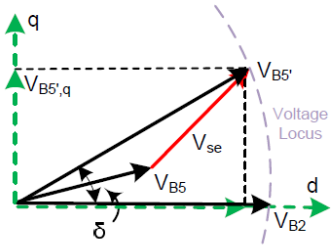

Fig. 2. Vector diagram of the series voltage V_{se} injection when the fault is on the $B5$ bus side.

III. THE PROPOSED CONTROL STRATEGY FOR VARIOUS OPERATIONAL STATES:

This section elaborates on the proposed transient management
scheme and the control strategy for the receiving end converter. The developed control system aims to achieve smooth power evacuation to the electric grid during steady state and fault conditions. The detailed explanation of the proposed control strategy for the shunt and series connections are provided below. The conventional double loop control strategy with fast inner current control and slower outer DC link and point of common coupling (PCC) voltage control loops is adopted for the shunt connection of the receiving end converter [18]. The inner current regulator of the shunt connection is developed in dq reference frame aligned with B5′ voltage based on the equations across the filter inductor as follows

$$\begin{cases} V_{g,d} = R_{f,sh} i_{sh,d} + L_{f,sh} \frac{di_{sh,d}}{dt} + V_{i,d} - L_{f,sh} \omega i_{sh,q} \\ V_{g,q} = R_{f,sh} i_{sh,q} + L_{f,sh} \frac{di_{sh,q}}{dt} + V_{i,q} + L_{f,sh} \omega i_{sh,d} \end{cases} \quad (1)$$

In equation (1) ish,d, ish,q, Vg,d, Vg,q,Vi,d and Vi,q are the d and q axis components of the inverter current, the filter voltage and the inverter voltage, respectively. During normal operation,the active current reference is determined based on the DC link voltage regulation loop, while the reactive current is used to regulate the PCC voltage to its nominal value. The series
controller injects zero voltage during the normal operation of the grid.
During the grid fault condition, the series converter provides the voltage across the series transformer in such a way to isolate the grid fault and to evacuate the wind power to the healthy portion of the network. The fault detection algorithm
recognizes the fault once the instantaneous magnitude of either B5′ or B5 bus voltages goes below 0.85 pu. The directional
relays present in the system are utilized to identify the fault side across the series transformer, which, in turn, decides the
control philosophy of the series and shunt converters.The direct voltage control is implemented for the series connection, which consists of the inner loop of the series controller.Based on the fault location, the series control is realized
in the reference frame aligned with either B4 or B2 voltages.The outer loop of the series converter is used to determine the
reference values for the voltage restoration. Based on the fault location, two different control strategies are realized. For better
visualization and understanding, two possible fault locations across both sides of the series transformer are examined in the
below subsections. A. Fault in the Grid 1 side of the series transformer
In Fig. 1, the fault is initiated at the bus B5, which causes a voltage dip at that bus. The series voltage injection aims to restore the magnitude of the B5′ bus voltage to 1 pu with an angle _ that will ensure the necessary active power evacuation to the Grid 2. The active power flowing from the B5′ bus to the Gird 2 is given as

$$P_{Grid2} = \frac{V_{B2} V_{B5'}}{X_{25'}} sin(\delta) \quad (2)$$

In (2), _ is the angle between voltages at buses B2 and B5′.By controlling this angle the active power delivered to the Grid 2 can be regulated, achieving a smooth power evacuation form the VSC-HVDC system. The vector diagram of the voltage
restoration and the necessarily series voltage injection can be clearly visualized from Fig. 2. The faulted B5 bus voltage
is subject to the magnitude decrease and may experience the phase angle jump. In this case, the series converter control is realized in the reference frame aligned with the B2 bus voltage. As it can be observed from Fig. 2, in this reference frame the q axis component of the B5′ voltage, Vq,B5′, can regulate the angle between the voltages at buses B5′ and B2.To achieve this, a control strategy is proposed and shown in Fig. 3, where the q axis reference of the voltage at B5′ is determined according to (3) based on the outer DC-link voltage regulation loop.

$$V_{B5',q,ref} = (V_{DC} - V_{DC,ref}) G_{se,PI} \quad (3)$$

In (3), VDC and VDC,ref are the measured and reference DC link voltages, while Gse,PI is the transfer function of the
respective PI regulator. For instance, if during a fault the active power is not fully evacuated from the DC link, it will cause
DC link voltage rise, which, in turn will increase the angle.This will lead to more active power flow from B5′ to Grid 2, and thus, the DC link overvoltage will be avoided.The d axis component reference is used to ensure the unity voltage regulation of the B5′ bus. Therefore, it is determined
according to the (4).

$$V_{B5',d,ref} = \sqrt{V_{B5'}^2 - V_{B',q,ref}^2} \quad (4)$$

During both steady state and transient operations, the onshore shunt converter control is realized in the reference frame aligned with the B5′ voltage. Hence, the transformation angle sh is acquired from VB5′ as shown in Fig. 4. The detailed
control diagram of the shunt and series interfaces and the generation of the modulation signals for the NSC is depicted in Fig. 3. To achieve both positive and negative sequence voltage injection, the Proportional-Resonant (PR) controllers are used in the series control system together with PI controllers as shown in Fig. 3. Whereas the implementation of the PR
controller is according to [19] with the transfer function given in (5)

$$G_{PR} = K_p + \frac{2K_i \omega_c s}{s^2 + 2\omega_c s + \omega^2} \quad (5)$$

In (5), the desired harmonic frequency ! is tuned at a double fundamental frequency to tackle the negative sequence voltage
injection requirement, whereas the !c is used to regulate thebandwidth of the controller. It is worthy to notice that the
series PI and PR controllers are deactivated during the normal operation by multiplying their inputs and outputs to zero. This is done to hinder the accumulation of the steady state error as the series part is only connected during grid faults. Similarly,
the outer loop PI controllers of the shunt part are deactivatedduring fault condition (Fig.3).

For the control of the shunt and series interfaces of the NSC, the 120◦ discontinuous modulation can be expressed by the following equations [20].

$$V_{se,abc}^m = V_{se,abc,ref}^m + [1 - max(V_{se,abc,ref}^m)] \quad (6)$$

$$V_{sh,abc}^m = V_{sh,abc,ref}^m + [(-1) - min(V_{sh,abc,ref}^m)] \quad (7)$$

In Fig. 3, the upper clumping of the series modulation reference is realized by using (6), where V mse,abc is the discontinued
modulation signal supplied to the three phase PWM generator.Similarly, equation (7) is used to generate the shunt reference
signal V msh,abc to be supplied to the PWM generator.
As the voltage across the shunt terminals does not see any changes during the faults in the Grid 2 side, therefore, in this case the shunt reference active current is switched from DC voltage regulation and set to its rated value to ensure the total active power evacuation from the VSC-HVDC system.
This helps to avoid the conflicting between the DC link voltage regulation loops of the shunt and series controllers.The reactive current is set to zero as the magnitude of the B5′voltage is regulated by the series voltage injection to 1 pu.
B. Fault in the Grid 2 side of the series transformer:

When the fault happens in the Grid 2 (Fig.5), the series converter restores the B5 bus voltage to 1 pu with such angle so that the wind power will be evacuated to Grid.The regulation of the angle between buses B5 and B4 allows controlling the power delivered to the Grid. In this scenario,the shunt converter can inject reactive power to support the faulty grid, which enhances the post fault voltage recovery.In Fig. 6, similar to the previous case, the series voltage is injected in such a way as to restore the voltage magnitude and angle between two consequent buses to ensure the necessary active power control. It can be noticed that in this case the voltage at bus B4 should be communicated to realize therequired control action and to inject the proper series voltage.The series reference frame is aligned with the B4 bus voltage as illustrated in Fig. 6.

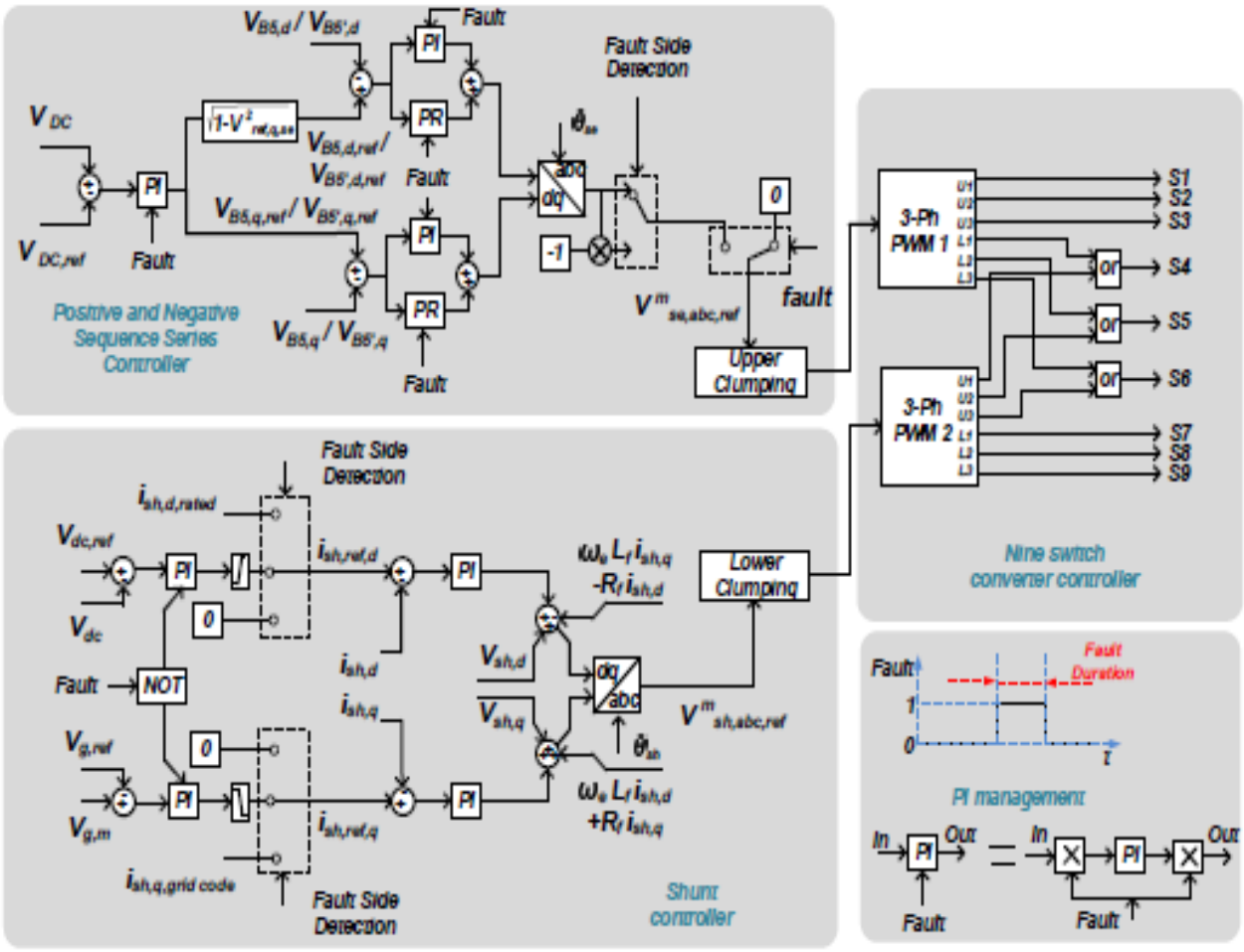

Fig. 3. Detailed control diagram of NSC for the proposed VSC-HVDC application

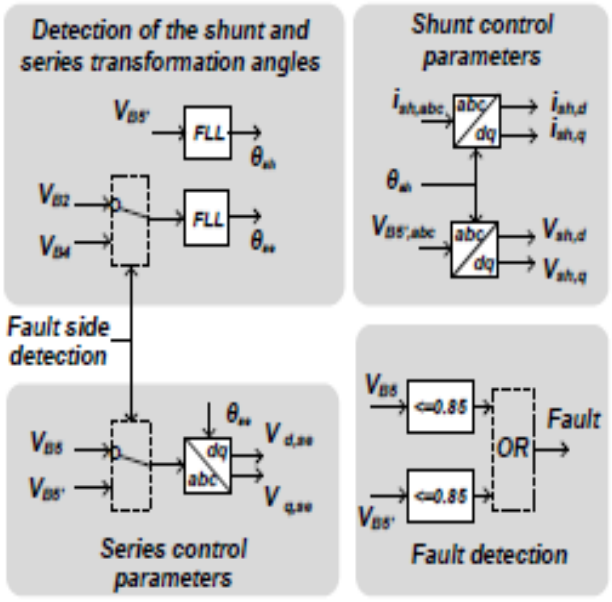

Fig. 4. Fault detection and data acquisition for the onshore shunt and series controller

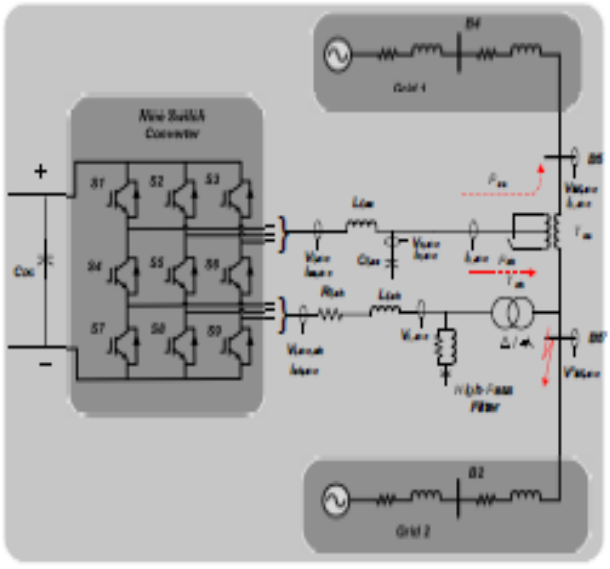

Fig. 5. Detailed diagram of NSC for shunt and series compensation for VSC-HVDC application when the system is subject to fault at $B5'$ bus.

The series voltage references are determined based on the outer DC link voltage regulation loop and the magnitude regulation block as in the previous case.

However, in this case, the shunt part is connected to the faulty part of the grid. Therefore, active power evacuation through the shunt terminal is not possible due to the voltage dip at bus B5′. Therefore, in this scenario, the shunt active current reference is set to zero. While the reactive current reference is determined in accordance with the grid code requirements.It is worth to note that based on the fault side, the series reference voltage vector should be flipped to ensure

bidirectionalvoltage restoration capability of the series converter. The redirection is done by multiplying the reference signals with(-1) as depicted in Fig. 3.

C. Series interface modeling:

The series controller consists of inner direct voltage control implemented in the synchronous reference frame aligned with either B4 bus or B2 bus and the outer DC link voltage control loops. The three phase voltages and currents of the series interface shown in Fig. 5 are given by

$$\begin{cases} i_{g,abc} = i_{se,abc} - i_{c,abc} = i_{se,abc} - C_{f,se}\frac{dV_c}{dt} \\ V_C = V_{i,abc} - L_{f,se}\frac{di_{se,abc}}{dt} \end{cases} \quad (8)$$

where VC is the voltage across the series filter capacitor. Transforming the equations (8) to dq synchronous reference frame, positive and negative sequence voltage and current components can be expressed as follows

$$\begin{cases} i^{\pm}_{g,d} = i^{\pm}_{se,d} - C_{f,se}\frac{dV^{\pm}_{c,d}}{dt} + \omega C_{f,se}V_{c,q}^{\pm} \\ i^{\pm}_{g,q} = i^{\pm}_{se,q} - C_{f,se}\frac{dV^{\pm}_{c,q}}{dt} - \omega C_{f,se}V_{c,d}^{\pm} \end{cases} \quad (9)$$

$$\begin{cases} V^{\pm}_{C,d} = V^{\pm}_{i,d} - L_{f,se}\frac{di^{\pm}_{se,d}}{dt} + \omega L_{f,se}i^{\pm}_{se,q} \\ V^{\pm}_{C,q} = V^{\pm}_{i,q} - L_{f,se}\frac{di^{\pm}_{se,q}}{dt} - \omega L_{f,se}i^{\pm}_{se,d} \end{cases} \quad (10)$$

For the simplicity of the derivation, only d axis component of
the positive sequence voltage is considered. By transferring(10) into Laplace domain and defining Vc,dig,d= rg , the following is derived

$$V_{i,d}(s) = s^2 C_{f,se}L_{f,se}V_{c,d}(s) - s2C_{f,se}L_{f,se}\omega V_{c,q}(s) + s\frac{L_{f,se}}{r_g}V_{c,d}(s) + V_{C,d}(s)(1-\omega^2 C_{f,se}L_{f,se}) - \omega L_{f,se}i_{g,q}(s) \quad (11)$$

The term rg is determined by the operation point of the system and for fast inner direct voltage control loop can be assumed constant. To tune the controllers, the (11) is
linearized around an operating point by adding small signal perturbations
ˆVi,d (s), ˆig,q (s), ˆ V c,q (s). Taking into account that 2Cf,seLf,se! ≪Lrg, (12) is derived as follows

$$\hat{V}_{i,d}(s) = \hat{V}_{c,d}(s)\left(s^2 C_{f,se}L_{f,se} + s\frac{L_{f,se}}{r_g} + (1-\omega^2 C_{f,se}L_{f,se})\right) \quad (12)$$

Hence, the plant transfer function for the direct series compensation becomes

$$G_{se}(s) = \frac{\hat{V}_{c,d}(s)}{\hat{V}_{i,d}(s)} = \frac{1}{s^2 C_{f,se}L_{f,se} + s\frac{L_{f,se}}{r_g} + (1-\omega^2 C_{f,se}L_{f,se})} \quad (13)$$

The PWM controlled VSC is modeled as an ideal transformer with the time delay equal to the dead time Td. Therefore, the
closed loop transfer function of the direct voltage control is as per (14).

$$T_{se}(s) = \frac{\hat{V}_{c,d,pu}(s)}{\hat{V}^{*}_{c,d,pu}(s)} = \frac{(K_{p,se} + \frac{K_{1,se}}{s})G_{se}(s)V_{dc}}{2V_{base}(sT_d + 1) + (K_{p,se} + \frac{K_{1,se}}{s})G_{se}(s)V_{dc}} \quad (14)$$

Fig. 7 depicts the Bode plot of the closed loop system, where it can be observed that the direct voltage control loop has infinite gain margin while the phase margin is equal to 119deg. Considering one bus ahead synchronous reference frame alignment for the series controller implementation and taking into account (14), it can be noticed that the series interface operation is lightly dependent on the total grid strength.However, it is worthy to point out that it is dependent on the impedance between two consequent buses used for the series control realization.

IV. SIMULATION RESULTS:

This section presents the evaluation of the proposed topology and transient management scheme for tackling severe
system faults in various locations of the onshore AC grid. The comparison of the NSC based topology and the conventional
system equipped with DC chopper is carried out to verify the former's performance. Simulations are carried out in the Matlab/ Simulink environment using the SimPowerSystem Toolbox.

A. PERFORMANCE IN RESPONSE TO THREE PHASE-TO-GROUND FAULTS IN THE B5 BUS SIDE:

In the first scenario, a three phase-to-ground fault is initiated at bus B5. It can be observed from Fig. 9 that the B5
bus voltage goes to almost zero, while the series controller regulates the series voltage injection in such a way to restorethe magnitude of the B5′ bus voltage to 1 pu with an angle between the buses B5′ and B2. The smooth voltage restoration of the VB5′ voltage can be observed from Fig. 9.
It can be seen from Fig. 10 that the angle difference between the voltages VB5′,A and VB2,A increased from 1.2◦ to 3◦. This
allows injecting the wind power through shunt terminals to the Gird 2 as shown in Fig. 11. It can be noticed that no significant
power is transferred through the series connection as the whole wind power is injected through the shunt interface. The
offshore station continues delivering the rated power generated.

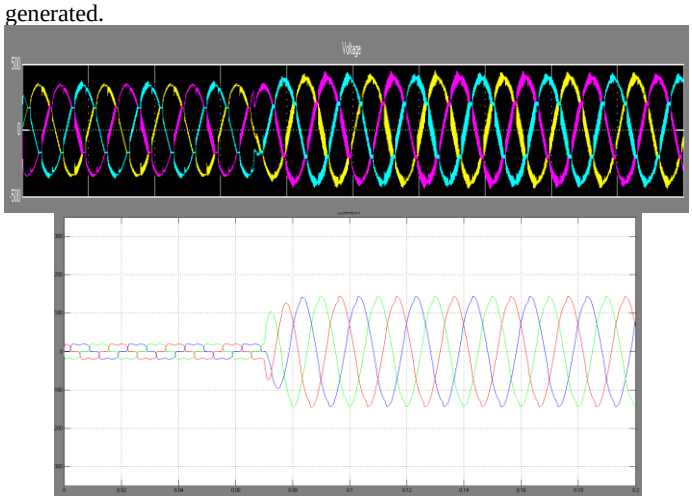

in theWF as can be observed in Fig. 11, which ensures that the WF is almost not affected by the severe fault in the onshore AC grid. If the active power was not evacuated from the DC link, then its voltage would quickly rise, the rising time determined by the equation (19)
t =C_V 2dc2_P(19).

In (19), C is the DC capacitance, _P is the mismatch of the power received at the onshore station and not delivered
to the grid, and _Vdc is the allowed DC link overvoltage. In this study the DC chopper starts its operation once the DC
link overvoltage at the receiving end converter reaches 10 % of its nominal value [2], [22]. Considering the charging time of capacitors at both sending and receiving end stations and considering the system parameters, it can be seen from (19) that it takes around one cycle to reach the maximum

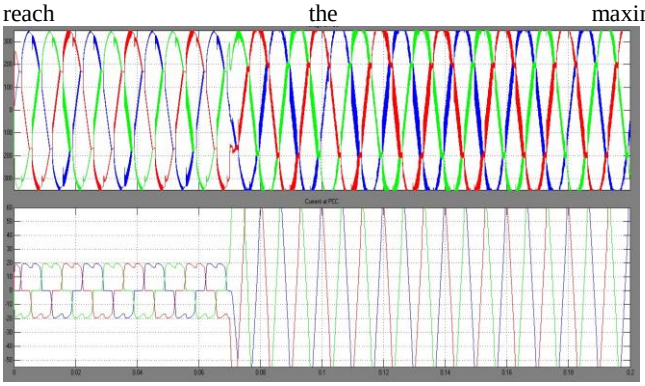

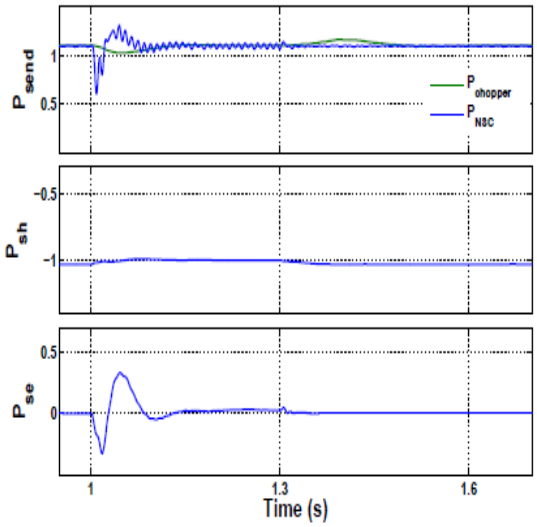

Fig. 15. Active powers delivered from the sending end converter P_{send} and injected though the shunt P_{sh} and series P_{se} interfaces during double line-to-ground fault in the $B5$ bus side.

DC link voltage. This can be confirmed from Fig. 12, where it takes around a cycle after fault detection for the DC chopper to start the power dissipation and regulation of the DC link voltage to 1.1 pu.With the proposed configuration, the DC link voltage of the receiving end converter (blue line) is regulated to1 pu, ensuring that the voltage at sending end converter is also regulated to little higher than 1 pu to allow necessary power flow from wind farm to the onshore grid. Because the total active power is evacuated by the onshore station, there is no overvoltage observed in the DC link as illustrated in Fig. 12.The series and shunt currents are presented in Fig. 13. Once the fault is initiated, the transient response of the series interface causes a slight DC shift in the series current. However, the transient DC bias quickly dies out as can be seen in Fig. 13.Due to the fact that in this scenario the active power evacuation is mainly continuous to be done through shunt terminal, the currents on the shunt side does not experience much transient.Both shunt and series currents are within the allowed rating.

B. PERFORMANCE IN RESPONSE TO DOUBLE LINE-TO-GROUND FAULT IN THE B5 BUS SIDE:

To demonstrate the capability of the proposed control scheme to tackle unbalanced faults in the Grid 1 side and to ensure smooth power delivery to the other part of the grid,a double line-to-ground fault is initiated at B5. It can be seen from Fig. 14 that the addition of the compensation voltage Vse
with the grid voltage, while the FLL allows doing the same in less than one cycle. The series controller is realized in the reference frame aligned with VB4 voltage. It can be observed from Fig. 19 that even after two cycles after grid disturbance the sin(_, se) with PLL is not locked with the VB4 voltage, while FLL allows almost ideal locking by that time. This results in better series controller action and less oscillations in the series delivered power as shown in Fig. 19. As discussed in the previous section, the shunt active current reference is set to zero in this scenario. Therefore, it can be examined from Fig. 19 that the shunt active power delivery decreases from rated power to almost zero during the fault. Simultaneously, the active power flow through the series terminal reaches to the rated power during the fault duration. It can be noticed that with both DC chopper and NSC equipped systems the offshore grid power evacuation is almost similar, so that, there

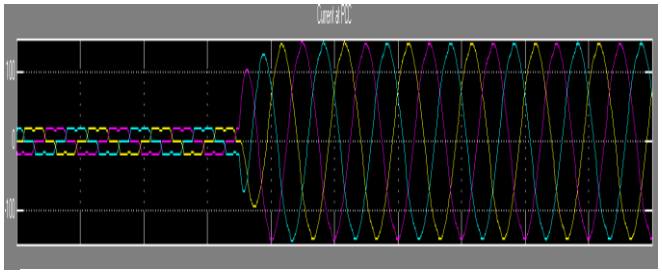

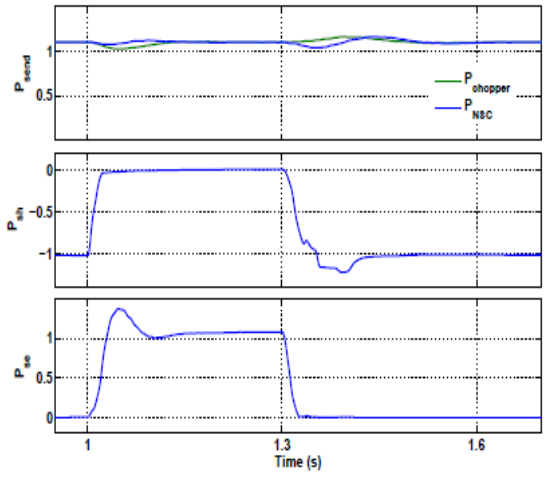

Fig. 23. Active powers delivered from the sending end converter P_{send} and injected though the shunt P_{sh} and series P_{se} interfaces during double line-to-ground fault in the $B5'$ bus side.

is no significant transient in the sending end active power. Fig.20, depicting the sending and receiving end DC link voltages,is self-explanatory. Due to the selected control approach, the maximum active current that the series part experiences is when the total power is evacuated through series interface.As the active power received from WPP does not exceed 1pu, therefore, to regulate the DC link voltage the series part needs to evacuate 1 pu power. This is forced by the DC link controller, which strives to maintain power balance. Therefore, he series active current does not exceed the maximum rating in all

scenarios. Whereas for the shunt part the current limiter ensures that the shunt currents are within the rated limits. In this scenario the shunt converter provides the grid support by
injecting the grid code specified reactive current. As it can be seen in Fig. 21, both shunt and series currents do not exceed the converter rated current.

D. PERFORMANCE IN RESPONSE TO DOUBLE LINE-TO-GROUND FAULT IN THE B5' BUS SIDE:

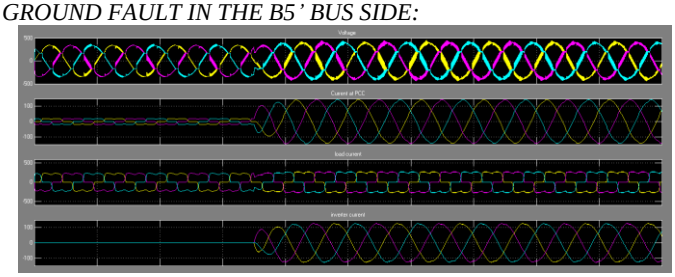

The performance of the implemented system during the double line-to-ground fault on B5′ bus between phases A and B is shown in Fig. 22. The unbalanced nature of the double line-to-ground fault can be observed from the trace of VB5′.The unbalanced voltage injection Vse during the double line to- ground fault shows the ability to provide both positive and negative-sequence voltage compensation. The voltage at theVB5 is undisturbed. Hence one portion of the grid is isolated from the double line-to-ground fault. This ensures the power evacuation through the series connection as shown in Fig. 23.After the fault clearance, the power evacuation is achieved through shunt terminals as can be observed from the Psh trace. It can be observed from Fig. 24 that in this case as well the proposed configuration maintains nominal DC link voltage during almost whole fault duration. In this scenario the shunt terminal voltage has an unbalanced profile. Therefore, the shunt currents also contain unbalanced component. Due to the feedforward voltage addition in the shunt controller, this component is not as much as unbalanced voltage component, which leads to relatively low shunt power oscillations. After fault clearance the shunt current is allowed to reach 1.1 pu for fast DC link voltage regulation. For this scenario the series interface experiences a slight overloading as its current reaches to 1.4 pu. This is due to the fact that in addition to full active power the series part provides reactive power support to the grid. For such scenarios the overloading capability of the IGBT switches might be employed, which is acceptable according to the leading converter manufacturers.

E. STABILITY TEST ON THE MATLAB/ SIMULINK 29 BUS TEST SYSTEM:

The stable operation of the system is enhanced by continuous delivery of the bulk power from wind farm to the grid as well as grid voltage profile enhancement. If the series voltage is not injected during fault condition, due to the low grid voltage the supply of the offshore wind power to the grid will be disturbed. Moreover, during fault condition without voltage restoration the generators also accelerate due to the imbalance between mechanical and electrical powers at the generator. To clearly illustrate this, the proposed topology was customized to the 29 bus dynamic test system available in the MATLAB/ Simulink as a demo model, where the detailed parameters of the system can be accessed in [25]. The test system comprising of seven synchronous generators, onshore wind farm and NSC-HVDC interconnected offshore wind farm
is depicted in Fig. 28. The response of the proposed system to the three phase fault at bus B5 was compared with the response of the similar system with conventional DC chopper based VSC-HVDC interconnection. The faulted grid voltage profile can be examined on the left side of Fig. 26, where voltages at several buses are shown. Whereas the right side of the Fig.26 clearly illustrates that with the NSC based solution the voltage profile is enhanced at all buses except the faulted bus B5. It is worthy to notice that B5' bus voltage is the same as B5 bus voltage for the chopper base solution. While with the NSC based system, once the fault is detected at bus B5, the series voltage injection restores the voltage at bus B5 (blue line on Fig. 26). The voltage restoration with an appropriate phase angle with respect to bus B2 voltage allows to evacuate the total active power supplied from offshore wind farm towards the B2 bus. The smooth power evacuation from

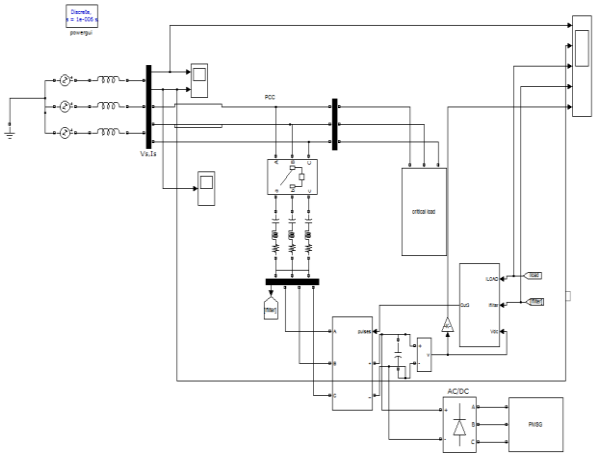

the HVDC system as well as the enhancement of the voltage profiles at the generators terminals prevents generators from acceleration. As in [10], the onshore system generators rotors speeds are considered for the system stability evaluation. Fig.27 illustrates that with the NSC based solution the generators rotor speeds oscillate during the fault duration from t=4s to t=4.3 s. As the fault is cleared, the oscillations die out and the system remains in the stable operation. On the same figure the response of the system with DC chopper is depicted to clearly illustrate the enhancement of the system stability with the proposed NSC based compensation system.

V. CONCLUSION:

This paper introduces a new configuration and control strategy for the VSC based HVDC link connecting offshore wind farms. A Nine Switch Converter is realized to achieve enhanced operation of the VSC-HVDC connected system by providing shunt and series compensation simultaneously in response to symmetrical and asymmetrical grid faults. An onshore station is modified to ensure power evacuation during onshore AC faults. The developed compensation strategy restores a voltage profile in one portion of the onshore grid and ensures the total active power evacuation into the healthy portion. Therefore, it increases the system stability in response to grid disturbances. In addition, the developed strategy for connecting wind farms through an NSC based VSC-HVDC system assists in reducing fault current contributions in the faulty network. A comprehensive simulation study has verified the effectiveness of the proposed scheme in enhancing the FRT operation of the offshore WFs.

TABLE I
SYSTEM PARAMETERS OF THE PROPOSED CONFIGURATION FOR VSC-HVDC BASED SYSTEM

Rated power	800 MVA	Series filter inductor	15 mH
DC link voltage	300 kV	Series filter capacitor	15 μF
Converter rated voltage	150 kV	Injection transformer	800 MVA
Onshore gird voltage	230 kV Hz	Shunt filter inductor	17 mH
Grid 1 SCR	20	Shunt filter resistance	0.01 Ω
Grid 1 X/R ratio	7	HPF Quality Factor	15
Grid 2 SCR	20	HPF Reactive Power	360 kVA
Grid 2 X/R ratio	7	HPF 1 Cutoff	2500 Hz
DC link capacitance	5 mF	HPF 2 Cutoff	5000 Hz
Onshore grid frequency	50 Hz	Shunt trans. rating	800 MVA
Offshore WF rating	800 MVA	Shunt transformer L	17 mH

REFERENCES:

[1] S. K. Chaudhary, R. Teodorescu, and P. Rodriguez, "Wind farm grid integration using vsc based hvdc transmission-an overview," in Energy 2030 Conference, 2008. ENERGY 2008. IEEE. IEEE, 2008, pp. 1–7.

[2] C. Feltes, H. Wrede, F. W. Koch, and I. Erlich, "Enhanced fault ridethrough method for wind farms connected to the grid through vsc-based hvdc transmission," IEEE Trans. Power Syst., vol. 24, no. 3, pp. 1537–1546, 2009.

[3] J. M. Carrasco, L. G. Franquelo, J. T. Bialasiewicz, E. Galv´an, R. C. P.Guisado, M. ´A. M. Prats, J. I. Le´on, and N. Moreno-Alfonso, "Powerelectronic systems for the grid integration of renewable energy sources:A survey," Industrial Electronics, IEEE Transactions on, vol. 53, no. 4,pp. 1002–1016, 2006.

[4] T. D. Vrionis, X. I. Koutiva, N. A. Vovos, and G. B. Giannakopoulos,"Control of an hvdc link connecting a wind farm to the grid for fault ride-through enhancement," IEEE Trans. Power Syst., vol. 22, no. 4, pp.2039–2047, 2007.

[5] L. Xu, L. Yao, and C. Sasse, "Grid integration of large dfig-based wind farms using vsc transmission," IEEE Trans. Power Syst., vol. 22, no. 3,pp. 976–984, 2007.

[6] G. Ramtharan, A. Arulampalam, J. B. Ekanayake, F. Hughes, and N. Jenkins, "Fault ride through of fully rated converter wind turbineswith ac and dc transmission," Renewable Power Generation, IET, vol. 3, no. 4, pp. 426–438, 2009.

[7] I. Erlich, C. Feltes, and F. Shewarega, "Enhanced voltage drop control by vsc hvdc systems for improving wind farm fault ridethrough capability," IEEE Trans. on Power Del., vol. 29, no. 1, pp. 378–385, Feb 2014.

[8] S. K. Chaudhary, R. Teodorescu, P. Rodriguez, and P. Kjar, "Chopper controlled resistors in vsc-hvdc transmission for wpp with full-scale converters," in Sustainable Alternative Energy (SAE), 2009 IEEE PES/IAS Conference on. IEEE, 2009, pp. 1–8.

[9] B. Silva, C. L. Moreira, H. Leite, and J. A. P. Lopes, "Control strategies for ac fault ride through in multiterminal hvdc grids," IEEE Trans. Power Del., vol. 29, no. 1, pp. 395–405, Feb 2014.

[10] A. A. van der Meer, M. Ndreko, M. Gibescu, and M. A. M. M. van der Meijden, "The effect of frt behavior of vsc hvdc-connected offshore wind power plants on ac/dc system dynamics," IEEE Trans. Power Del., vol. 31, no. 2, pp. 878-887, April 2016.

[11] A. Moawwad, M. S. El Moursi, W. Xiao, and J. L. Kirtley, "Novel configuration and transient management control strategy for vsc-hvdc," IEEE Trans. Power Sys., vol. 29, no. 5, pp. 2478–2488, 2014.

[12] A. Moawwad, M. S. El Moursi, and W. Xiao, "Advanced fault ridethrough management scheme for vsc-hvdc connecting offshore windfarms," IEEE Trans. Power Syst., vol. PP, no. 99, pp. 1–12, 2016.

[13] O. D. Adeuyi, M. Cheah-Mane, J. Liang, L. Livermore, and Q. Mu, "Preventing dc over-voltage in multi-terminal hvdc transmission," CSEE Journal of Power and Energy Systems, vol. 1, no. 1, pp. 86–94, March2015.

[14] N. R. Chaudhuri, R. Majumder, and B. Chaudhuri, "System frequency support through multi-terminal dc (mtdc) grids," IEEE Trans. on PowerSyst., vol. 28, no. 1, pp. 347–356, Feb 2013.

[15] X. Zhao and K. Li, "Adaptive backstepping droop controller design for multi-terminal high-voltage direct current systems," IET Generation, Transmission Distribution, vol. 9, no. 10, pp. 975–983, 2015.

[16] J. Arrillaga, High voltage direct current transmission. Iet, 1998, no. 29.

[17] P. Hao, W. Zanji, and C. Jianye, "Study on the control of shunt active dc filter for hvdc systems," IEEE Trans. Power Del., vol. 23, no. 1, pp. 396–401, Jan 2008.

[18] L. He, C. C. Liu, A. Pitto, and D. Cirio, "Distance protection of ac grid with hvdc-connected offshore wind generators," IEEE Trans. Power Del., vol. 29, no. 2, pp. 493–501, April 2014.

[19] R. Teodorescu, F. Blaabjerg, M. Liserre, and P. C. Loh, "Proportional resonant controllers and filters for grid-connected voltage-source converters,"in Electric Power Applications, IEE Proceedings, vol. 153, no. 5. IET, 2006, pp. 750–762.

[20] L. Zhang, P. C. Loh, and F. Gao, "An integrated nine-switch power conditioner for power quality enhancement and voltage sag mitigation," 0885-8977 (c) 2016 IEEE.

[21] Ali, A. Nazar. "Cascaded Multilevel Inverters for Reduce Harmonic Distortions in Solar PV Applications." Asian Journal of Research in Social Sciences and Humanities 6.Issue : 11 (2016): 703-715.

[22] Ali, A. Nazar. "A Single phase Five level Inverter for Grid Connected Photovoltaic System by employing PID Controller." African journal of Research 6.1 (2011): 306-315.

[23] ali, A.Nazar. "A SINGLE PHASE HIGH EFFICIENT RANSFORMERLESSINVERTER FOR PV GRID CONNECTED POWER SYSTEM USING ISPWM TECHNIQUE." International Journal of Applied Engineering Research 10.ISSN 0973-4562 (2015): 7489-7496.

[24] Ali, A. Nazar. "Performance Enhancement of Hybrid Wind/Photo Voltaic System Using Z Source Inverter with Cuk-sepic Fused Converter." Research Journal of Applied Sciences, Engineering and Technology 7.ISSN: 2040-7459; (2014): 3964-3970.

[25] Ali, A. Nazar. "Ride through Strategy for a Three-Level Dual Z-Source Inverter Using TRIAC." Scientific Research publication 7.ISSN Online: 2153-1293 (2016): 3911-3921.

[26] Ali, A. Nazar. "An ANFIS Based Advanced MPPT Control of a Wind-Solar Hybrid Power Generation System." International Review on Modelling and Simulations 7.ISSN 1974-9821 (2014): 638-643.

[27] Nazar Ali, A. "Performance Analysis of Switched Capacitor Multilevel DC/AC Inverter using Solar PV Cells." International Journal for Modern Trends in Science and Technology 3.05 (2017): 104-109.

[28] Ali, A.Nazar. "FPGA UTILISATION FOR HIGH LEVELPOWER CONSUMPTION DRIVES

BASEDONTHREE PHASE SINUSOIDAL PWM -VVVF CONTROLLER." International Journal of Communications and Engineering 4.Issue: 02 (2012): 25-30.

[29] ali, A.Nazar. "A SINGLE PHASE HIGH EFFICIENT TRANSFORMERLESS INVERTER FOR PV GRID CONNECTED POWER SYSTEM USING ISPWM TECHNIQUE." International Journal of Applied Engineering Research 10.ISSN 0973-4562 (2015): 7489-7496.

[30] JAIGANESH, R. "Smart Grid System for Water Pumping and Domestic Application using Arduino Controller." International Journal of Engineering Research & Technology (IJERT) 5.13 (2017): 583-588.

[31] Pau1l, M. Mano Raja, R. Mahalakshmi, M. Karuppasamypandiyan, A. Bhuvanesh, and R. Jai Ganesh."Classification and Detection of Faults in Grid Connected Photovoltaic System."

[32] Ganesh, Rajendran Jai, et al. "Fault Identification and Islanding in DC Grid Connected PV System." Scientific Research Publishing 7.Circuits and Systems, 7, 2904-2915. (2016): 2904-2915.

[33] Jaiganesh, R., et al. "Smart Grid System for Water Pumping and Domestic Application Using Arduino Controller." International Journal for Modern Trends in Science and Technology 3.05 (2017): 385-390.

[34] Kalavalli,C., et al. “Single Phase Bidirectional PWM Converter for Microgrid System.” International Journal of Engineering and Technology (IJET) ISSN : 0975-4024 Vol 5 No 3 Jun-Jul 2013.

[35] Lilly Renuka, R., et al. “Power Quality Enhancement Using VSI Based STATCOM for SEIG Feeding Non Linear Loads. ” International Journal of Engineering and Applied Sciences (IJEAS) ISSN: 2394-3661, Volume-2, Issue-5, May 2015.

[36] Karthikeyan,B. JEBASALMA. “RESONANT PWM ZVZCS DC TO DC CONVERTERS FOR RENEWABLE ENERGY APPLICATIONS .“International Journal of Power Control and Computation(IJPCSC)Vol 6. No.2 – Jan-March 2014 Pp. 82-89©gopalax Journals, Singaporeavailable at :www.ijcns.comISSN: 0976-268X.

[37] Gowri,N, et al. “Power Factor Correction Based BridgelessSingle Switch SEPIC Converter Fed BLDC

[38] Motor.”ADVANCES in NATURAL and APPLIED SCIENCES. ISSN: 1995-0772 AENSI PublicationEISSN: 1998-1090 http://www.aensiweb.com/ANAS2016 March 10(3): pages 190-197.

[39] Ramkumar,R., et al.” A Novel Low Cost Three Arm Ac AutomaticVoltage Regulator” ADVANCES in NATURAL and APPLIED SCIENCESISSN: 1995-0772 AENSI PublicationEISSN: 1998-1090 http://www.aensiweb.com/ANAS2016 March 10(3): pages 142-151.

[40] Kodeeswaran, S., T. Ramkumar, and R. Jai Ganesh. "Precise temperature control using reverse seebeck effect." In Power and Embedded Drive Control (ICPEDC), 2017 International Conference on, pp. 398-404. IEEE, 2017.

[41] Subramanian, AT Sankara, P. Sabarish, and R. Jai Ganesh. "An Improved Voltage follower Canonical Switching Cell Converter with PFC for VSI Fed BLDC Motor." Journal of Science and Technology (JST) 2, no. 10 (2017): 01-11.

[42] Murugesan.S, R. Senthilkumar."DESIGN OF SINGLE PHASE SEVEN LEVEL PV INVERTER USING FPGA."International Journal of Emerging Technology in Computer Science & Electronics, 2016, Vol.20, No.2, pp.207-2012.

[43] S. Murugesan, C. Kalavalli, " FPGA Based Multilevel Inverter With Reduce Number of Switches For Photovoltaic System", International Journal of Scientific Research in Science, Engineering and Technology(IJSRSET), Print ISSN : 2395-1990, Online ISSN : 2394-4099, Volume 3 Issue 6, pp.628-634, September-October 2017.

[44] Vikram, A. Arun, R. Navaneeth, M. Naresh Kumar, and R. Vinoth. "Solar PV Array Fed BLDC Motor Using Zeta Converter For Water Pumping Applications." Journal of Science and Technology (JST) 2, no. 11 (2017): 09-20.

[45] Nagarajan, L. Star Delta Starter using Soft Switch for Low Power Three Phase Induction Motors. Australian Journal of Basic and Applied Sciences, 9(21), 175-178.

[46] Vinusha, S., & Nagarajan, L. (2015). CURRENT SOURCE INVERTER FED INDUCTION MOTOR DRIVE USING MULTICELL CONVERTER WITH ANFIS CONTROL.

[47] Nagarajan, L., & Nandhini, S. (2015). AN EFFICIENT SOLAR/WIND/BATTERY HYBRID SYSTEM WITH HIGH POWER CONVERTER USING PSO.

[48] Subramanian, AT Sankara, P. Sabarish, and R. Jai Ganesh. "An Improved Voltage follower Canonical Switching Cell Converter with PFC for VSI Fed BLDC Motor." Journal of Science and Technology (JST) 2.10 (2017): 01-11.

[49] Compensator, D. S. (2015). AN ADAPTIVE CONTROL AND IMPROVEMENT OF POWER QUALITY IN GRID CONNECTED SYSTEM USING POWER ELECTRONIC CONVERTERS.

[50] Sabarish, P., Sneha, R., Vijayalakshmi, G., & Nikethan, D. (2017). Performance Analysis of PV-Based Boost Converter using PI Controller with PSO Algorithm. Journal of Science and Technology (JST), 2(10), 17-24.

[51] T.Vishnu Kumar, V. Suresh Kumar, T. Sumeet, M.Srimaha “Hybrid Front end Interface DC-DC Converter with ANFIS Based Control of EMS System”. International Journal of Scientific Research in Science and Technology, Volume 3, Issue 8, Print ISSN: 2395-6011, 2017.

[52] T. Vishnu kumar, V. Suresh Kumar, A new approach to front end interface DC-DC converter” International Journal of Multidisciplinary Research and Modern Education (IJMRME) ISSN(online): 2454-6119 Volume I, Issue II, 2015

[53] V.Suresh kumar, T. Vishnu kumar, A certain investigation for the battery charging system” International Journal of Multidisciplinary Research and Modern Education (IJMRME) ISSN(online): 2454-6119 Vol.1 Issue.1 2015.

[54] S.Enimai, S.Jayanthi, T.Vishnu kumar Isolated Power System Design Using Modified P&O Technique” Middle-East Journal of Scientific Research 24 (S2): 150-156, 2016, ISSN 1990-9233